

# High-order perturbation expansion of non-Hermitian Floquet theory for multiphoton and above-threshold ionization processes

Dmitry A. Telnov\* and Shih-I Chu

*Department of Chemistry, University of Kansas, and Kansas Center for Advanced Scientific Computing, Lawrence, Kansas 66045*

(Received 16 July 1999; published 14 December 1999)

A high-order perturbation theory is presented for efficient and accurate computation of multiphoton and above-threshold ionization cross sections of atoms and molecules in weak to medium strength laser fields. The procedure is based on a Raleigh-Schrödinger perturbative expansion of the time-independent non-Hermitian Floquet Hamiltonian. The reduced Green function and generalized pseudospectral discretization techniques are extended to facilitate the calculation of complex quasienergy resonance states without the need of diagonalizing the full Floquet Hamiltonian. Explicit expressions are presented for the determination of intensity-dependent total and partial rates and electron angular distributions. The theory is applied to a case study of multiphoton detachment of  $H^-$  for a range of laser frequencies (corresponding to the absorption of a minimum of two photons) and laser intensities from  $10^7$  to  $10^{12}$  W/cm<sup>2</sup>. It is found that a 16th-order perturbative Floquet procedure provides an excellent description of the two-photon-dominant detachment processes for laser intensity up to  $2 \times 10^{11}$  W/cm<sup>2</sup>. The predicted electron angular distributions are in good agreement with recent experimental data.

PACS number(s): 32.80.Rm, 32.80.Fb, 42.50.Hz

## I. INTRODUCTION

As early as 1975, Rescigno, McCurdy, and McKoy (RMM) [1,2] have outlined a method for calculating (one-photon, weak-field) atomic and molecular photoabsorption cross sections using a discrete  $L^2$  basis set expansion and the complex scaling technique [3]. The method has the advantage that it allows the calculation to be performed directly at the physical energies of interest and relies on no second procedure to construct the cross section. The most recent application of this procedure includes, for example, the accurate calculation of photoabsorption of Li, involving three active electrons and the use of the complex scaling saddle-point technique [4]. However, the extension of the RMM procedure [1,2] to the multiphoton case has not been discussed so far. In principle, the non-Hermitian Floquet formalism [5,6] can be applied to the calculation of multiphoton absorption cross sections of atoms and molecules in both weak and strong fields [6,7]; the procedure, however, involves the determination of the complex quasienergy states from the whole Floquet matrix. The motivations of this paper are twofold. First, we outline a procedure that works for both weak and intermediate laser intensities but does not require the diagonalization of the full Floquet matrix. Second, the method will not only provide an extension of the RMM method to the multiphoton and above-threshold ionization regime but also allow the examination of the intensity-dependent behavior of electron angular distributions and partial rates in multiphoton detachment processes.

Our procedure is based on a high-order Rayleigh-Schrödinger perturbative expansion of the time-independent non-Hermitian Floquet Hamiltonian and the use of the re-

duced Green-function technique. We note that an earlier attempt to make the connection of the Floquet matrix approach with the conventional continued-fraction expansion of resolvent matrix elements has been presented by Maquet, Chu, and Reinhardt [8] by means of the successive formal iteration of the Brillouin-Wigner expansion but no explicit implementation procedure and application has been made. Moreover, instead of using the  $L^2$  basis set expansion techniques as in all the previous RMM-type calculations, we have adopted here the complex-scaling generalized pseudospectral (CSGPS) method [9] for the discretization of the Hamiltonian and the determination of the complex quasienergy resonances. As demonstrated in various recent atomic and molecular resonance calculations [9–11], the CSGPS method is simple to implement and computationally highly efficient and accurate.

The organization of this paper is as follows. In Sec. II, we present a high-order perturbative expansion of the non-Hermitian Floquet Hamiltonian and introduce the reduced Green-function technique for the calculation of the successive higher-order complex quasienergy resonances. In Sec. III, we present the explicit expressions for the calculation of generalized cross sections for multiphoton ionization or detachment. In Sec. IV, the lowest-order perturbation theory for the electron angular distributions and partial rates for above-threshold multiphoton detachment is presented. Finally in Sec. V, we apply the procedure to the study of intensity- and frequency-dependent multiphoton detachment of  $H^-$ . Comparison with the recent experimental data will be made.

## II. HIGH-ORDER PERTURBATION THEORY FOR NON-HERMITIAN FLOQUET HAMILTONIAN AND COMPLEX QUASIENERGY RESONANCES

In this section, we start from a brief review of the non-Hermitian Floquet formalism [5–7]. Then we present a de-

---

\*Permanent address: Institute of Physics, St. Petersburg State University, 198904 St. Petersburg, Russia.

tailed  $N$ th-order perturbative analysis of the non-Hermitian Floquet Hamiltonian and explicit formulas for the determination of complex quasienergy resonances.

Consider an atomic or molecular system subject to the external time-dependent field. The total Hamiltonian  $\hat{H}(t)$  is a sum of the unperturbed Hamiltonian  $\hat{H}^{(0)}$  and the interaction term  $\hat{H}^{(1)}(t)$  due to the external field:

$$\hat{H}(t) = \hat{H}^{(0)} + \hat{H}^{(1)}(t). \quad (1)$$

The (many-body) wave function of the system depends on the coordinates of all particles as well as on time. We shall use the notation  $\mathbf{r}$  for all the coordinates. The wave function  $\Psi(\mathbf{r}, t)$  satisfies the time-dependent Schrödinger equation (in atomic units):

$$i \frac{\partial}{\partial t} \Psi(\mathbf{r}, t) = \hat{H}(t) \Psi(\mathbf{r}, t). \quad (2)$$

If the external field is periodic in time,

$$\hat{H}^{(1)}(t+T) = \hat{H}^{(1)}(t), \quad (3)$$

where  $T$  is the period, one can seek the solution of Eq. (2) in the form of the Floquet state:

$$\Psi(\mathbf{r}, t) = \exp(-i\varepsilon t) \psi(\mathbf{r}, t), \quad (4)$$

$$\psi(\mathbf{r}, t+T) = \psi(\mathbf{r}, t), \quad (5)$$

where  $\varepsilon$  is the quasienergy. Expanding the time-periodic wave function  $\psi(\mathbf{r}, t)$  and the external field  $\hat{H}^{(1)}(t)$  in Fourier series

$$\psi(\mathbf{r}, t) = \sum_{m=-\infty}^{\infty} \exp(-im\omega t) \psi_m(\mathbf{r}), \quad (6)$$

$$\hat{H}^{(1)}(t) = \sum_{m=-\infty}^{\infty} \exp(-im\omega t) \hat{H}_m^{(1)}, \quad (7)$$

one arrives at the following set of time-independent coupled equations for the Fourier components  $\psi_m(\mathbf{r})$ :

$$(\hat{H}^{(0)} - m\omega) \psi_m(\mathbf{r}) + \sum_{n=-\infty}^{\infty} \hat{H}_{m-n}^{(1)} \psi_n(\mathbf{r}) = \varepsilon \psi_m(\mathbf{r}). \quad (8)$$

Equation (8) is an eigenvalue problem for the quasienergy  $\varepsilon$ . For the special case of electric dipole coupling in the linearly polarized monochromatic field,

$$\hat{H}^{(1)}(t) = - \sum_j (\mathbf{F} \cdot \mathbf{r}_j) \cos \omega t, \quad (9)$$

the summation in Eq. (8) contains only  $n=m$ ,  $m \pm 1$  terms. In the general case the quasienergy  $\varepsilon$  is complex valued:

$$\varepsilon = E - i \frac{\Gamma}{2}, \quad (10)$$

where  $E$  (the real part of the quasienergy) describes the position of the shifted energy level in the external field, and  $\Gamma$  is the total ionization or multiphoton ionization rate. One can rewrite Eq. (8) in the form of the Floquet Hamiltonian eigenvalue problem:

$$\hat{H}_F \vec{\psi} = \varepsilon \vec{\psi}, \quad (11)$$

where  $\vec{\psi}$  represents the vector composed of the Fourier components  $\psi_m(\mathbf{r})$ , and the Floquet Hamiltonian  $\hat{H}_F$  is defined by the left-hand side of Eq. (8).

To facilitate solving Eq. (11) for the complex quasienergies, we perform the complex-scaling transformation [3]:

$$\mathbf{r} \rightarrow \mathbf{r} \exp(i\beta) \quad (12)$$

(only radial coordinates are affected by this transformation;  $\beta$  is the angle of complex rotation). Upon this transformation, the Floquet Hamiltonian  $\hat{H}_F(\mathbf{r} \exp(i\beta)) \equiv \hat{H}_F(\beta)$  becomes non-Hermitian [complex symmetric if the unrotated Hamiltonian  $\hat{H}_F(\mathbf{r})$  is real], and the wave functions  $\psi_m(\mathbf{r} \exp(i\beta))$  become squared integrable. One can further perform an expansion of the Fourier components  $\psi_m(\mathbf{r} \exp(i\beta))$  on the basis of the angular momentum eigenstates, and a basis set expansion (or generalized pseudospectral grid discretization [9]) of the remaining functions depending on the radial coordinates  $r$ . Then the solution of the Floquet Hamiltonian problem reduces to a *complex matrix* eigenvalue problem. We shall use the notation  $H_F$ ,  $H_0$ , and  $V$  for the *complex-rotated* total Floquet Hamiltonian matrix, unperturbed Floquet Hamiltonian matrix, and perturbation matrix, respectively. The notation  $\psi$  will be used for the complex-rotated eigenvector. The non-Hermitian Floquet formalism and its generalizations have been extensively applied to the study of atomic and molecular multiphoton processes in strong fields in the last two decades [5–7, 10–12].

We now extend the Rayleigh-Schrödinger perturbation theory [13] to the non-Hermitian Floquet Hamiltonian matrix eigenvalue problem:

$$H_F(\beta) \psi(\beta) = \varepsilon \psi(\beta), \quad (13)$$

where  $H_F = H_0 + V$ . We suppose that the eigenvalue problem for the unperturbed (complex-rotated) matrix  $H_0$ ,

$$H_0 \psi_k^{(0)} = \varepsilon_k^{(0)} \psi_k^{(0)}, \quad k=0, 1, 2, \dots, \quad (14)$$

is solved, so the unperturbed eigenvalues  $\varepsilon_k^{(0)}$  and eigenvectors  $\psi_k^{(0)}$  are available, the latter subject to the following *biorthonormal* relation:

$$\langle \psi_k^{(0)} | \psi_n^{(0)} \rangle = \delta_{kn}. \quad (15)$$

Note that the inner product in Eq. (15) is defined in such a way that in the coordinate representation only the angular part of  $\psi_k^{(0)}$  is complex conjugated but not its radial part. Let  $k=0$  correspond to the state under consideration (the theory is not restricted to the ground state,  $k=0$  can correspond to any state). Then the perturbed eigenvector  $\psi_0$  and eigenvalue  $\varepsilon_0$  for this selected state can be written as

$$\psi_0 = \psi_0^{(0)} + \sum_{n=1}^{\infty} \psi_0^{(n)}, \quad (16)$$

$$\varepsilon_0 = \varepsilon_0^{(0)} + \sum_{n=1}^{\infty} \varepsilon_0^{(n)}. \quad (17)$$

The expansions (16) and (17) are the perturbation theory expansions, and the terms  $\varepsilon_0^{(n)}$  and  $\psi_0^{(n)}$  represent the  $n$ th order of the perturbation theory. The expansions (16) and (17) are unique provided the following biorthonormal relation is satisfied:

$$\langle \psi_0 | \psi_0^{(0)} \rangle = 1 \quad (18)$$

or

$$\langle \psi_0^{(n)} | \psi_0^{(0)} \rangle = 0, \quad n = 1, 2, \dots \quad (19)$$

(the corrections to the eigenvector are biorthogonal to the unperturbed eigenvector for any order of the perturbation theory). Substituting Eqs. (16) and (17) in Eq. (13) and collecting the terms of the same order, one arrives at the following recursive procedure to calculate the quantities  $\varepsilon_0^{(n)}$  and  $\psi_0^{(n)}$ :

$$(H_0 - \varepsilon_0^{(0)}) \psi_0^{(n)} = \langle \psi_0^{(0)} | V | \psi_0^{(n-1)} \rangle \psi_0^{(0)} - V \psi_0^{(n-1)} + \sum_{m=1}^{n-1} \varepsilon_0^{(m)} \psi_0^{(n-m)}, \quad (20)$$

$$\varepsilon_0^{(n)} = \langle \psi_0^{(0)} | V | \psi_0^{(n-1)} \rangle, \quad n \geq 2. \quad (21)$$

The recursive procedure starts with the initial terms for  $n = 1$  which are as follows:

$$(H_0 - \varepsilon_0^{(0)}) \psi_0^{(1)} = \langle \psi_0^{(0)} | V | \psi_0^{(0)} \rangle \psi_0^{(0)} - V \psi_0^{(0)}, \quad (22)$$

$$\varepsilon_0^{(1)} = \langle \psi_0^{(0)} | V | \psi_0^{(0)} \rangle. \quad (23)$$

The inhomogeneous equations (20) and (22) can be solved with the help of the reduced Green-function matrix  $G$ . It is defined by the following expansion on the basis of the unperturbed eigenvectors:

$$G = \sum_{k \neq 0} \frac{|\psi_k^{(0)}\rangle \langle \psi_k^{(0)}|}{\varepsilon_k^{(0)} - \varepsilon_0^{(0)}}. \quad (24)$$

Note that the term with  $k=0$  is missing in the sum in Eq. (24), so  $G$  is a regular matrix in the case when the eigenvalue  $\varepsilon_0^{(0)}$  is not degenerate. The reduced Green matrix  $G$  can be easily constructed if all the eigenvectors and eigenvalues of the unperturbed (complex-rotated) Hamiltonian matrix  $H_0$  are available. Using the matrix  $G$  to solve Eqs. (20) and (22), one can write

$$\psi_0^{(1)} = -GV\psi_0^{(0)}, \quad (25)$$

$$\psi_0^{(n)} = -GV\psi_0^{(n-1)} + \sum_{m=1}^{n-1} \varepsilon_0^{(m)} G \psi_0^{(n-m)}, \quad n \geq 2. \quad (26)$$

Now we take into account the structure of the unperturbed (complex-rotated) Floquet Hamiltonian matrix  $H_0$ . First, it is a block-diagonal matrix with respect to the Floquet Fourier index  $m$  [see Eq. (8)]:

$$[H_0]_{mm'} = (h_0 - m\omega) \delta_{mm'}, \quad (27)$$

where  $h_0$  is the field-free atomic (molecular) Hamiltonian matrix and  $\omega$  is the external field frequency. The theory outlined above is exact for the general many-body problem. The following details (to the end of this section) apply only for the one-electron problem where the unperturbed Hamiltonian possesses spherical symmetry. Extension to the many-electron case is straightforward. When using the angular momentum eigenstates basis set described above, the atomic Hamiltonian matrix  $h_0$  is also block diagonal, each block corresponding to the angular momentum  $l$ :

$$[h_0]_{ll'} = h_{0,l} \delta_{ll'}, \quad (28)$$

( $h_{0,l}$  is the radial Hamiltonian matrix for the angular momentum  $l$ ). Thus the eigenvalues and eigenvectors can be enumerated with three indexes, the first of them corresponding to the atomic radial eigenstate ( $j$ ), the second one to the angular momentum ( $l$ ), and the third one to the Floquet Fourier index ( $m$ ) (we assume that the external perturbation possesses the axial symmetry like in the case of linearly polarized laser field, so the projection of the angular momentum onto the field axis is conserved and equal to that of the initial unperturbed state). Hence in the perturbation theory expressions above one has to make the following substitutions:

$$\varepsilon_k^{(0)} \equiv \varepsilon_{j,l,m}^{(0)}, \quad (29)$$

$$\psi_k^{(0)} \equiv \psi_{j,l,m}^{(0)}. \quad (30)$$

The eigenvalues  $\varepsilon_{j,l,m}^{(0)}$  are related to the eigenvalues  $E_{j,l}$  of the atomic Hamiltonian  $h_0$  [see Eq. (27)]:

$$\varepsilon_{j,l,m}^{(0)} = E_{j,l} - m\omega. \quad (31)$$

We assume that the initial state  $\psi_0^{(0)}$  corresponds to  $j=j_0$ ,  $l=l_0$ , and  $m=0$ . Consider the vector space of dimension  $N \times L \times M$  where  $N$  is the number of radial eigenstates (the number of radial grid points when using pseudospectral discretization),  $L$  is the number of angular momentum blocks, and  $M$  is the number of photon blocks retained in the Floquet Hamiltonian matrix  $H_0$ . Then the eigenvectors  $\psi_{j,l,m}^{(0)}$  have a block structure in this space just like the structure of the matrix  $H_0$ :

$$[\psi_{j,l,m}^{(0)}]_{m'} = \psi_{j,l}^{(0)} \delta_{mm'}, \quad (32)$$

$$[\psi_{j,l}^{(0)}]_{l'} = \phi_{j,l}^{(0)} \delta_{ll'}. \quad (33)$$

Here the vectors  $\psi_{j,l}^{(0)}$  and  $\phi_{j,l}^{(0)}$  have dimensions  $N \times L$  and  $N$ , respectively. The vector  $\phi_{j,l}^{(0)}$  is a field-free atomic radial eigenvector corresponding to the angular momentum  $l$  and the radial quantum number  $j$ . Substituting the expressions (31), (32), and (33) into Eq. (24), one arrives at the block-diagonal structure of the reduced Green-function matrix  $G$ :

$$[G]_{jlm,j'l'm'} = \sum_{i=0}^{N-1} \frac{[\phi_{i,l}^{(0)}]_j [\phi_{i,l}^{(0)}]_{j'}}{E_{i,l} - \varepsilon_0^{(0)} - m\omega} \delta_{mm'} \delta_{ll'}. \quad (34)$$

Here  $[\phi_{i,l}^{(0)}]_j$  are the components of the unperturbed atomic radial eigenvector, the indices  $m$  and  $m'$  span the interval  $[M_s, M_f]$  (such that  $M_f - M_s + 1 = M$  and the point  $m=0$  is included), the indices  $l$  and  $l'$  vary within the interval  $[0, L-1]$ , and the indices  $j$  and  $j'$  vary within the interval  $[0, N-1]$ . Equation (34) is valid in general except for the  $m=0, l=l_0$  case. In this special case the sum does not include  $i=j_0$ :

$$[G]_{j'l_0, j'l_0} = \sum_{\substack{i=0 \\ i \neq j_0}}^{N-1} \frac{[\phi_{i,l_0}^{(0)}]_j [\phi_{i,l_0}^{(0)}]_{j'}}{E_{i,l_0} - \varepsilon_0^{(0)}}. \quad (35)$$

As one can see, the reduced Green-function matrix  $G$  has a simple block structure that facilitates performing matrix-vector multiplication in Eq. (26). The dimension of this matrix can be decreased by a factor 2 if the perturbation has a definite spatial parity, as is the case for the dipole interaction with the external field. In this case the perturbation matrix  $V$  couples  $m$  with  $m \pm 1$  and  $l$  with  $l \pm 1$ . For example, if the unperturbed state has  $l=0$ , then even Floquet blocks of the reduced Green-function matrix contain only even angular momenta, and the odd Floquet blocks contain only odd angular momenta. For the linearly polarized external field with the field strength  $\mathbf{F}$  and frequency  $\omega$ , the perturbation time-dependent operator is  $-(\mathbf{F} \cdot \mathbf{r}) \cos \omega t$ . The photon and angular blocks of the corresponding complex-rotated matrix  $V$  appear as follows:

$$V_{lm,l'm'} = \frac{-Fr \exp(i\beta)}{2\sqrt{(2l+1)(2l'+1)}} (l\delta_{l,l'+1} + l'\delta_{l,l'-1}) \times (\delta_{m,m'+1} + \delta_{m,m'-1}). \quad (36)$$

The radial structure of the matrix  $V$  depends on the basis set used to expand the radial functions. For the pseudospectral discretization of the radial coordinate  $r$  [9], the matrix  $V$  is diagonal with respect to the radial index  $j$ :

$$V_{jlm,j'l'm'} = \frac{-Fr_j \exp(i\beta)}{2\sqrt{(2l+1)(2l'+1)}} \delta_{jj'} (l\delta_{l,l'+1} + l'\delta_{l,l'-1}) \times (\delta_{m,m'+1} + \delta_{m,m'-1}), \quad (37)$$

$r_j$  being the radial pseudospectral grid points.

With the reduced Green-function matrix  $G$  defined by Eqs. (34) and (35), and the perturbation matrix  $V$  defined by Eqs. (36) and (37), one can construct the  $n$ th-order correction

to the quasienergy eigenvector according to Eq. (26) and the  $n$ -order correction to the complex quasienergy according to Eq. (21).

### III. PERTURBATIVE EXPRESSIONS FOR GENERALIZED CROSS SECTIONS IN MULTIPHOTON IONIZATION OR DETACHMENT PROCESSES

Due to parity restrictions for the dipole interaction, the power series (17) for the perturbed complex eigenvalue  $\varepsilon$  contains only even powers of the external field  $F$  and can be written as follows:

$$\varepsilon_0 = \varepsilon_0^{(0)} + \sum_{n=1}^{\infty} \alpha_{2n} F^{2n}. \quad (38)$$

The coefficients  $\alpha_{2n}$  represent hyperpolarizabilities and depend on the frequency of the external field. They are real numbers for  $n < n_0$  and complex numbers for  $n \geq n_0$  where  $n_0$  is the minimal number of photons required for electron detachment. The coefficients  $\alpha_{2n}$  can be represented as  $2n$ th-order corrections to the quasienergy  $\varepsilon_0^{(2n)}$  if one assumes  $F=1$  in the definition of the perturbation [see, e.g., Eqs. (36) and (37)]:

$$\alpha_{2n} = \varepsilon_0^{(2n)}|_{F=1} = \langle \psi_0^{(0)} | V | \psi_0^{(2n-1)} \rangle|_{F=1}. \quad (39)$$

Note that our coefficient  $\alpha_2$  is related to the conventional dipole polarizability  $\alpha$  as follows:

$$\alpha_2 = -\frac{1}{4}\alpha. \quad (40)$$

The real part of the complex quasienergy  $\varepsilon$  in Eq. (38) yields the shift of the energy level in the external field whereas the imaginary part describes the (multiphoton) ionization or detachment rate (the rate  $\Gamma$  is equal to minus doubled the imaginary part of  $\varepsilon$ ).

The photon flux  $J$  corresponding to the electric field strength  $F$  and frequency  $\omega$  is calculated according to

$$J = \frac{cF^2}{8\pi\omega}, \quad (41)$$

$c$  being the velocity of light. The generalized cross section  $\sigma^{(n_0)}$  of  $n_0$ -photon-dominant detachment is defined as the ratio of the total (multiphoton) ionization or detachment rate  $\Gamma$  and  $n_0$ th power of the photon flux  $J$ :

$$\sigma^{(n_0)} = \frac{\Gamma}{J^{n_0}}. \quad (42)$$

Note that the expression (42) is valid for both weak and strong fields. In the weak field limit,  $\sigma^{(n_0)}$  becomes independent of the field intensity, and only the term with  $n=n_0$  in

the right-hand side of Eq. (38) is to be included. The detachment rate  $\Gamma$  in this limit can be written as follows:

$$\Gamma = -2F^{2n_0} \text{Im}(\alpha_{2n_0}), \quad (43)$$

and the generalized cross section  $\sigma^{(n_0)}$  can be expressed through the hyperpolarizability coefficient  $\alpha_{2n_0}$ :

$$\sigma^{(n_0)} = -2 \left( \frac{8\pi\omega}{c} \right)^{n_0} \text{Im}(\alpha_{2n_0}). \quad (44)$$

The generalized cross sections may be expressed in terms of the matrix elements involving the unperturbed (complex-rotated) initial-state wave function, reduced Green function, and the perturbation operator. For example, the one- and two-photon (weak-field) ionization or detachment cross sections are given by

$$\sigma^{(1)} = \frac{16\pi\omega}{c} \text{Im}(\langle \psi_0^{(0)} | VGV | \psi_0^{(0)} \rangle |_{F=1}), \quad (45)$$

$$\sigma^{(2)} = 2 \left( \frac{8\pi\omega}{c} \right)^2 \text{Im}(\langle \psi_0^{(0)} | VGVGVGV | \psi_0^{(0)} \rangle |_{F=1} - \langle \psi_0^{(0)} | VGV | \psi_0^{(0)} \rangle \langle \psi_0^{(0)} | VG^2V | \psi_0^{(0)} \rangle |_{F=1}). \quad (46)$$

Note that Eqs. (45) and (46) are not restricted to the perturbation form (36) and can be applied to many-body systems as well. Equation (45) reproduces, in a different notation, the result obtained by Rescigno and McKoy [1] for the one-photon case. Expression (46) is the generalization of RMM theory to the two-photon case, and so on. For the one-electron system with the spherical-symmetric unperturbed Hamiltonian, the reduced Green-function matrix  $G$  and the perturbation matrix  $V$  are given by Eqs. (34) and (36), respectively. The (bra) radial wave functions in Eqs. (45) and (46) must not be complex conjugated, and the radial integrations are performed with the complex-rotated unperturbed wave function  $\psi_0$  corresponding to the complex-rotated Hamiltonian  $H_0$ . For example, in the case of one-photon detachment of the initial  $s$  state (the unperturbed radial eigenfunction  $\phi_{j_0,0}$  and unperturbed energy  $E_{j_0,0}$ ), the cross section (45) can be recast in a simple form involving the radial integrations only:

$$\sigma^{(1)} = \frac{4\pi\omega}{3c} \text{Im} \left( \sum_{i=0}^{N-1} \frac{\langle \phi_{j_0,0}^{(0)} | r \exp(i\beta) | \phi_{i,1}^{(0)} \rangle \langle \phi_{i,1}^{(0)} | r \exp(i\beta) | \phi_{j_0,0}^{(0)} \rangle}{E_{i,1} - E_{j_0,0} - \omega} \right). \quad (47)$$

Again, it is assumed in Eq. (47) that the inner products involve the complex-rotated radial eigenfunctions  $\langle \phi |$  without complex conjugation.

#### IV. LOWEST-ORDER PERTURBATION THEORY FOR THE ELECTRON ANGULAR DISTRIBUTIONS IN ABOVE-THRESHOLD DETACHMENT OF NEGATIVE IONS

We consider the electron energy and angular distributions for a multiphoton above-threshold detachment of negative ions such as  $\text{H}^-$ , which can be accurately described by the one-electron model potential [14]. The general nonperturbative expression in our previous Floquet calculations [12,15,16] will be employed:

$$\frac{d\Gamma_n}{d\Omega} = (2\pi)^{-2} k_n |A_n|^2. \quad (48)$$

Here,

$$k_n = \sqrt{2[\text{Re } \varepsilon - (2\omega)^{-2}F^2 + n\omega]} \quad (49)$$

is the electron drift momentum, and the  $n$ -photon detachment amplitude  $A_n$  is defined as follows (linear polarization of the external field is assumed):

$$A_n = (2\pi)^{-1} \int_{-\pi}^{\pi} d\tau \exp[in\tau - i(2\omega)^{-3}F^2 \sin(2\tau) + i(\mathbf{k}_n \cdot \mathbf{F})\omega^{-2} \cos \tau] \int d\mathbf{r} \exp[-i(\mathbf{k}_n \cdot \mathbf{r}) + i(\mathbf{r} \cdot \mathbf{F})\omega^{-1} \sin \tau] W(\mathbf{r}) \psi(\mathbf{r}, \tau/\omega), \quad (50)$$

$\mathbf{F}$  and  $\omega$  being the laser field strength and frequency, respectively,  $W(\mathbf{r})$  being the electron-core interaction potential. The vector  $\mathbf{k}_n$  has the direction under which the ejected electrons are detected. Expression (48) is valid in the general nonperturbative case. Instead of using the perturbative expansion of Eq. (48), which can be tedious, we shall present here only the *lowest-order* perturbation theory (LOPT) for the electron angular distributions in the multiphoton above-threshold detachment processes, which is useful in the weaker field regime. That means we expand Eq. (48) in power series of  $F$  and retain only the lowest power of  $F$  for each number  $n$  of absorbed photons. Obviously, the  $n$ -photon detachment amplitude  $A_n$  within this approximation scales with the factor  $F^n$ . To obtain the LOPT approximation for  $A_n$ , note that the Fourier components of the quasienergy wave function  $\psi(\mathbf{r}, t)$  within LOPT also scale with the appropriate power of  $F$ , so the following equation holds:

$$\psi(\mathbf{r}, t) = \sum_{m=-\infty}^{\infty} F^{|m|} \chi_m(\mathbf{r}) \exp(-im\omega t). \quad (51)$$

Here the functions  $\chi_m(\mathbf{r})$  do not depend on  $F$ . They can be represented as a series on the basis of the Legendre polynomials depending on the angle  $\vartheta$  between  $\mathbf{r}$  and  $\mathbf{F}$ :

$$\chi_m(\mathbf{r}) = \sum_{l=0}^{\infty} \sqrt{l+1/2} \chi_{m,l}(r) P_l(\cos \vartheta). \quad (52)$$

Inserting Eqs. (51) and (52) into Eq. (50), making the expansion in powers of  $F$  and retaining only the lowest power for each  $n$ , one obtains the following LOPT result for the  $n$ -photon detachment amplitude  $A_n$ :

$$\begin{aligned} a_{n,l} = & 4\pi(2l+1) \sum_{n_1=0}^n \sum_{n_2=0}^n \sum_{n_3=0}^n \sum_{m=0}^n \delta_{n,2n_1+n_2+n_3+m} \frac{(-1)^{n_2} i^{n_3} (k_n^{(0)})^{n_3}}{n_1! 2^{4n_1+n_2+n_3} \omega^{3n_1+n_2+2n_3}} \\ & \times \sum_{l_2} \sum_{l_3} \frac{(2l_2+1)(2l_3+1)}{(n_2-l_2)!!(n_2+l_2+1)!!(n_3-l_3)!!(n_3+l_3+1)!!} \\ & \times \sum_{l_1=0}^n (2l_1+1) i^{-l_1} \begin{pmatrix} l & l_1 & l_3 \\ 0 & 0 & 0 \end{pmatrix}^2 \sum_{l_4=0}^n \begin{pmatrix} l_1 & l_2 & l_4 \\ 0 & 0 & 0 \end{pmatrix}^2 \sqrt{l_4+1/2} \int_0^\infty dr r^{2+n_2} j_{l_1}(k_n^{(0)} r) W(r) \chi_{m,l_4}(r). \end{aligned} \quad (54)$$

In Eq. (54),

$$\begin{pmatrix} l_1 & l_2 & l_3 \\ 0 & 0 & 0 \end{pmatrix}$$

stands for the Wigner  $3j$  symbol;  $j_l(x)$  is the spherical Bessel function. The sums over  $l_2$  and  $l_3$  span the intervals from 0 to  $n_2$  and from 0 to  $n_3$ , respectively. They include only even values for even  $n_2$  and  $n_3$ , and only odd values for odd  $n_2$  and  $n_3$ , respectively. The ejected electron momentum  $k_n^{(0)}$  within LOPT is defined as

$$k_n^{(0)} = \sqrt{2(\varepsilon_0 + n\omega)}. \quad (55)$$

The integration with respect to the radial coordinate  $r$  in Eq. (54) is performed along the real axis  $r$ , so the back-rotation procedure [17] can be used to obtain the wave function for real values of the radial coordinate. Although Eq. (54) contains multiple summations, it is easy to program and compute. In the one-photon case, an explicit form of Eq. (54) for the initial  $s$  state reads as

$$\begin{aligned} a_{1,1} = & i\pi\sqrt{2} \left[ \frac{k_1^{(0)}}{\omega^2} \int_0^\infty dr r^2 j_0(k_1^{(0)} r) W(r) \chi_{0,0}(r) \right. \\ & + \frac{1}{\omega} \int_0^\infty dr r^3 j_1(k_1^{(0)} r) W(r) \chi_{0,0}(r) \\ & \left. - \sqrt{12} \int_0^\infty dr r^2 j_1(k_1^{(0)} r) W(r) \chi_{1,1}(r) \right]. \end{aligned} \quad (56)$$

$$A_n = F^n \sum_{l=0}^n a_{n,l} P_l(\cos \theta), \quad (53)$$

with  $\theta$  being the angle between  $\mathbf{k}_n$  and  $\mathbf{F}$ . Due to definite parity of the perturbation, the sum in Eq. (53) contains only even or odd angular momenta  $l$ , depending on the number of absorbed photons  $n$  and the initial state parity. The partial angular amplitudes  $a_{n,l}$  are defined as follows:

The LOPT angular distributions are calculated according to the following expression:

$$\frac{d\Gamma_n}{d\Omega} = \frac{k_n^{(0)}}{(2\pi)^2} F^{2n} \left| \sum_{l=0}^n a_{n,l} P_l(\cos \theta) \right|^2. \quad (57)$$

The partial rates  $\Gamma_n$  corresponding to absorption of  $n$  photons can be obtained by the integration of Eq. (57) over the whole angular range:

$$\Gamma_n = \frac{k_n^{(0)}}{2\pi} F^{2n} \sum_{l=0}^n \frac{2}{2l+1} |a_{n,l}|^2. \quad (58)$$

## V. A CASE STUDY: CALCULATIONS OF COMPLEX QUASIENERGIES AND ELECTRON ANGULAR DISTRIBUTIONS FOR MULTIPHOTON DETACHMENT OF $\text{H}^-$

We have performed the calculations for the negative ion  $\text{H}^-$  described by an accurate one-electron model [14]. It reproduces both the exact experimental binding energy [18] and the low-energy  $e - \text{H}(1s)$  elastic scattering phase shifts. The one-photon detachment cross sections based on this model potential are in excellent agreement with earlier accurate two-electron calculations [19,20]. Using this model potential, Wang *et al.* [21] have performed detailed nonperturbative Floquet studies of the frequency- and intensity-dependent multiphoton detachment of  $\text{H}^-$  and their results were in good agreement with the experimental data of Tang *et al.* [22]. Our recent nonperturbative Floquet study of the electron angular distributions associated with the above-threshold multiphoton detachment of  $\text{H}^-$  by 1064-nm laser

field [16] and that of the two-photon angular distributions near one-photon threshold [12], again using this model potential, is also in good harmony with the recent experimental work of Zhao *et al.* [23] and of Præstegaard *et al.* [24], respectively. In our recent nonperturbative Floquet studies [12,16,21], the CSGPS method [9] is used for the discretization and solution of the non-Hermitian Floquet Hamiltonian. The CSGPS method is found to be both accurate and computationally highly efficient and is applicable to both low-lying and highly excited atomic and molecular resonance states [9–11]. A detailed description of the uniform and exterior complex-scaling pseudospectral discretization can be found elsewhere [12]. In the present calculations we make use of the uniform CSGPS method.

Up to 100 radial grid points is used for CSGPS discretization, which is sufficient for full convergence of the complex quasienergies and eigenvectors to machine precision. For the highest (16th) order of the perturbation theory used in the present calculations, the number of angular momenta needed is 9 ( $l=0-8$ ). In the range of the validity of the perturbative method discussed here, the high-order perturbative Floquet procedure is computationally far less demanding than the full nonperturbative Floquet approach, since only the diagonalization of several unperturbed matrices (of different angular momentum) of small dimension (up to  $100 \times 100$ ) is needed. Moreover the same matrix information can be stored and used for the construction of the reduced Greenfunction matrices for different laser frequencies. In addition to the computational advantage, the perturbative Floquet approach also allows the examination of the intensity-dependent behavior of multiphoton processes order by order.

First, we have performed the calculations to determine the range of the laser field intensities where the perturbation theory applies. We have calculated the complex quasienergies and partial detachment rates for the fixed wavelength  $\lambda = 1.908 \mu\text{m}$  ( $\omega = 0.02388$  a.u.), used in experiment [24]. This wavelength corresponds to the two-photon-dominant detachment case ( $n_0 = 2$ ). The calculations have been performed for several intensities of the external field, using the present perturbative approach and nonperturbative Floquet method employed in our previous studies [12,16]. The results are shown in Table I for the complex quasienergies and in Table II for the partial rates. For the complex quasienergies, the full high-order perturbation theory of Sec. II was applied (maximum to the 16th order for higher intensities) whereas for the partial rates the LOPT of Sec. IV was used. As one can see from Table I, the high-order perturbative description is excellent for the intensities as high as  $2 \times 10^{11} \text{ W/cm}^2$ . For the highest intensity presented ( $2 \times 10^{11} \text{ W/cm}^2$ ) here, the 16th-order perturbative result is converged to five digits of accuracy for the level shift and within 0.03% for the width. This intensity is about the strongest intensity considered in the experiments [22] and [24].

We have also studied the higher-intensity cases. For laser intensity larger than  $4 \times 10^{11} \text{ W/cm}^2$ , the 16th-order perturbative calculation is not sufficient to achieve full converged results. For even higher intensity, other high-order resummation technique (such as Padé approximation) may be used to facilitate the convergence but this is not the focus of this

TABLE I. Complex quasienergies for two-photon-dominant detachment of  $\text{H}^-$  by  $1.908\text{-}\mu\text{m}$  radiation calculated for several intensities of the external field. (A), high-order perturbation theory (the notation A $q$  denotes perturbative calculation of  $q$ th order, LOPT corresponds to fourth order); (B), nonperturbative Floquet calculation. The numbers in square brackets indicate the powers of 10.

Laser intensity ( $\text{W/cm}^2$ )	Method	Quasienergy (a.u.)
$10^8$	LOPT	$-2.773335949[-02] - i2.427[-11]$
	A6	$-2.773335949[-02] - i2.426[-11]$
	B	$-2.773335949[-02] - i2.426[-11]$
$10^9$	LOPT	$-2.773516217[-02] - i2.42653[-09]$
	A8	$-2.773516217[-02] - i2.42386[-09]$
	B	$-2.773516217[-02] - i2.42386[-09]$
$10^{10}$	LOPT	$-2.775292889[-02] - i2.4265331[-07]$
	A10	$-2.775293498[-02] - i2.4000243[-07]$
	A12	$-2.775293498[-02] - i2.4000245[-07]$
	B	$-2.775293498[-02] - i2.4000245[-07]$
$10^{11}$	LOPT	$-2.790459699[-02] - i2.426534740[-05]$
	A12	$-2.790985494[-02] - i2.185196502[-05]$
	A14	$-2.790986912[-02] - i2.184610731[-05]$
	A16	$-2.790986518[-02] - i2.184791228[-05]$
	B	$-2.790986607[-02] - i2.184747633[-05]$
$2 \times 10^{11}$	LOPT	$-2.801767543[-02] - i9.706143057[-05]$
	A12	$-2.805327632[-02] - i7.969182454[-05]$
	A14	$-2.805509145[-02] - i7.894203597[-05]$
	A16	$-2.805408401[-02] - i7.940410991[-05]$
	B	$-2.805445135[-02] - i7.922490583[-05]$

paper. Alternatively one can simply extend the nonperturbative Floquet method for stronger field cases. We also note that the perturbative Floquet approach should be applicable to significantly larger intensity for neutral atoms and molecules since the electron-binding energies there are order(s) of magnitude larger than those of negative ions.

Table I contains also the LOPT results for the complex quasienergies (corresponds to the fourth-order perturbation theory for the two-photon detachment). As shown, the LOPT is adequate for laser intensity up to  $10^9 \text{ W/cm}^2$ , but it begins to show deviation from the nonperturbative results as the laser intensity approaches  $10^{10} \text{ W/cm}^2$ . At the intensity  $10^{11} \text{ W/cm}^2$  the discrepancy between LOPT and nonperturbative quasienergies is already quite significant, and the LOPT description of the total detachment rates becomes completely inadequate.

Table II shows the comparison of the partial rates calculated by the LOPT and nonperturbative Floquet method. Similar to the total rates, the LOPT is excellent for laser intensity less than  $10^9 \text{ W/cm}^2$  but becomes inadequate for intensity larger than  $10^{10} \text{ W/cm}^2$ .

In Figs. 1 and 2 we present the (weak-field) generalized

TABLE II. Partial detachment rates for above-threshold multiphoton detachment of  $H^-$  by 1.908- $\mu\text{m}$  radiation calculated for several intensities of the external field using LOPT (A) and nonperturbative Floquet approach (B). The numbers in square brackets indicate the powers of 10.  $n$  is the number of photons absorbed.

Laser intensity ( $\text{W}/\text{cm}^2$ )	Method	Partial detachment rates (a.u.)			
		2	3	4	5
$10^7$	A	4.853[−13]	2.213[−18]	8.283[−24]	3.056[−29]
	B	4.853[−13]	2.213[−18]	8.283[−24]	3.054[−29]
$10^8$	A	4.853[−11]	2.213[−15]	8.283[−20]	3.056[−24]
	B	4.852[−11]	2.213[−15]	8.283[−20]	3.056[−24]
$10^9$	A	4.853[−09]	2.213[−12]	8.283[−16]	3.056[−19]
	B	4.846[−09]	2.211[−12]	8.277[−16]	3.054[−19]
$10^{10}$	A	4.853[−07]	2.213[−09]	8.283[−12]	3.056[−14]
	B	4.778[−07]	2.191[−09]	8.223[−12]	3.037[−14]
$10^{11}$	A	4.853[−05]	2.213[−06]	8.283[−08]	3.056[−09]
	B	4.165[−05]	1.996[−06]	7.652[−08]	2.847[−09]
$2 \times 10^{11}$	A	1.941[−04]	1.771[−05]	1.325[−06]	9.779[−08]
	B	1.434[−04]	1.433[−05]	1.118[−06]	8.341[−08]

cross sections of multiphoton detachment calculated according to Eq. (44). The calculations were performed for three- and eight-photon detachment frequency ranges. Our present LOPT-Floquet results are in complete agreement with the previous calculations by Laughlin and Chu [14] obtained with the use of conventional perturbation theory and Dalgarno-Lewis procedure [25], using the same model potential for  $H^-$  [14]. The agreement demonstrates the numerical accuracy and convergence of the present perturbative Floquet procedure.

The dependence of the complex quasienergies on the intensity of the laser field is determined by the coefficients  $\alpha_{2n}$

[see Eq. (38)]. For the frequency range corresponding to the two-photon-dominant case ( $n_0=2$ ), the coefficients  $\alpha_{2n}$  are listed in Table III. The imaginary part of the coefficient  $\alpha_4$  can be used for calculations of the two-photon generalized cross section according to Eq. (44). Note that imaginary parts of higher hyperpolarizability coefficients ( $\alpha_6$  to  $\alpha_{10}$ ) are often positive. That means the contribution to the total detachment rate from the particular above-threshold detachment rate is overridden by the negative higher-order corrections to the above-threshold rates for lower number of photons absorbed. For example, the positive imaginary part of  $\alpha_6$  means that the contribution to the total rate from the three-

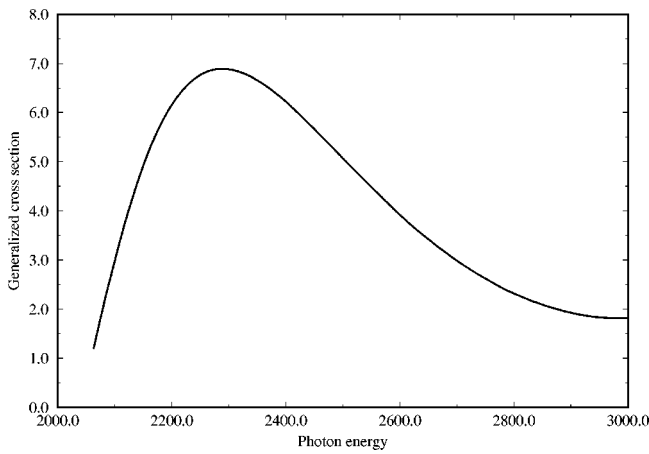


FIG. 1. Generalized cross section  $\sigma^{(3)}$  of three-photon detachment of  $H^-$  (in units of  $10^{-79} \text{ cm}^6 \text{ s}^2$ ) as a function of photon energy (in units of  $\text{cm}^{-1}$ ).

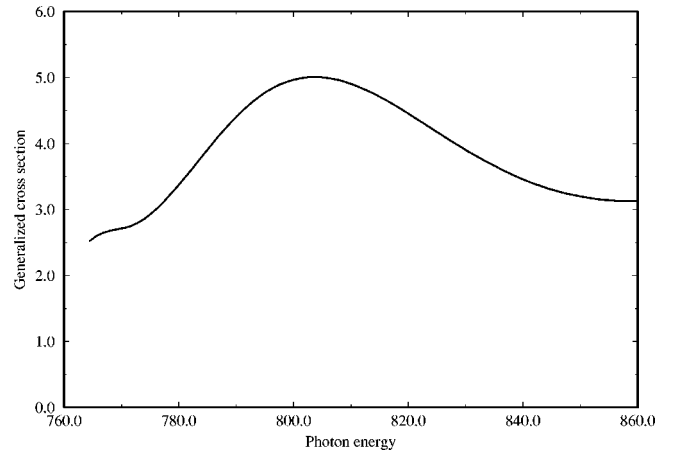


FIG. 2. Generalized cross section  $\sigma^{(8)}$  of eight-photon detachment of  $H^-$  (in units of  $10^{-230} \text{ cm}^{16} \text{ s}^7$ ) as a function of photon energy (in units of  $\text{cm}^{-1}$ ).



TABLE III. Hyperpolarizability coefficients  $\alpha_{2n}$  for multiphoton detachment of  $H^-$ . The frequency range corresponds to the minimum of two absorbed photons. The numbers in square brackets indicate the powers of 10.

Laser frequency (a.u.)	Coefficients $\alpha_{2n}$ (a.u.)				
	$\alpha_2$	$\alpha_4$	$\alpha_6$	$\alpha_8$	$\alpha_{10}$
0.014	-5.639[01]	-8.598[06] -i3.508[06]	-2.544[12] +i7.707[12]	-1.389[18] +i1.153[19]	-2.832[25] +i3.579[25]
0.015	-5.717[01]	-3.859[06] -i6.437[06]	-6.815[11] +i1.009[12]	-2.104[17] +i1.531[17]	-2.462[22] +i9.518[22]
0.017	-5.902[01]	-2.690[05] -i5.900[06]	-1.724[11] +i5.136[11]	+4.736[15] -i4.337[16]	-4.117[21] +2.687[21]
0.019	-6.134[01]	+1.425[06] -i5.019[06]	-2.241[11] +i3.587[11]	+1.914[16] -i1.972[16]	-1.283[21] +i7.472[20]
0.021	-6.431[01]	+2.508[06] -i4.132[06]	-2.510[11] +i2.272[11]	+1.661[16] -i9.433[15]	-9.092[20] +i5.188[20]
0.023	-6.824[01]	+3.284[06] -i3.313[06]	-2.593[11] +i1.415[11]	+1.572[16] -i5.669[15]	-1.007[21] +i4.123[20]
0.025	-7.374[01]	+4.025[06] -i2.613[06]	-2.928[11] +i9.160[10]	+2.060[16] -i4.420[15]	-1.798[21] +i4.225[20]
0.027	-8.263[01]	+5.440[06] -i2.045[06]	-5.354[11] +i6.639[10]	+8.156[16] -i5.775[15]	-1.821[22] +i1.210[21]

photon above-threshold detachment is completely reversed by the negative six-order contribution to the two-photon detachment rate.

The LOPT partial angular amplitudes  $a_{n,l}$  [Eq. (54)] for the same frequency range corresponding to  $n_0=2$  are presented in Table IV. Also shown are the weights in the partial detachment rate  $\Gamma_n$  of the electrons ejected with the particular angular momentum  $l$ . For the two-photon detachment, one can see how the weights of  $s$  and  $d$  electrons vary as the frequency increases. At the beginning of the frequency range, for the frequencies close to the two-photon threshold (0.013 87 a.u.), the weight of the  $s$  electrons is almost 100%, in accordance with the Wannier threshold law. With the frequency increasing, the weight of  $d$  electrons also increases, and at the end of the frequency range, in the vicinity of the one-photon threshold (0.027 73 a.u.), the situation is almost reversed. The  $d$  electrons constitute about 95% of the total population after two-photon detachment. This result was also obtained in our previous nonperturbative Floquet calculation [12] (for the intensities equal or less than  $10^{11}$  W/cm<sup>2</sup>) and confirmed experimentally [24]. The tendency is preserved for higher frequencies where one-photon detachment is possible. Our previous nonperturbative Floquet calculations of multiphoton detachment by 1064-nm radiation (well above the one-photon threshold) [16] also give about 90% of  $d$  electrons in the two-photon above-threshold rate.

For the above-threshold detachment (corresponding to three to five photons absorbed), the variation of the different angular momenta populations is not monotonous within the frequency range between the two-photon and one-photon thresholds. In general, the weight of the lowest angular momentum increases at the beginning of the frequency range, reaches its maximum, and then decreases as the frequency approaches the one-photon threshold. The behavior of the highest angular momentum population is opposite; first it decreases, reaches its minimum, and then increases. One can notice that for all above-threshold channels (three to five photons absorbed) the weight of the highest angular momentum is larger at the high-frequency end of the interval than at the low-frequency end.

In summary, we have presented a high-order perturbation Floquet approach for the calculation of the complex quasienergies and electron angular distributions. The method does not require the diagonalization of the full Floquet Hamiltonian matrix, and the block structure of the unperturbed Floquet Hamiltonian matrix greatly facilitates the calculations. The comparison of the perturbative and nonperturbative results in the model potential  $H^-$  calculations shows that the high-order perturbation theory description of the total detachment rates is adequate for weak and medium strong laser fields (up to the intensity  $2 \times 10^{11}$  W/cm<sup>2</sup> for the two-photon-dominant frequency range). The LOPT description of

TABLE IV. Partial angular amplitudes  $a_{n,l}$  for the above-threshold detachment of  $H^-$ . The frequency range corresponds to the minimum of two absorbed photons. The column “%” shows the percent weight of the electrons with the particular angular momentum in the partial detachment rate  $\Gamma_n$ . The numbers in square brackets indicate the powers of 10.

Laser frequency (a.u.)	Number of photons absorbed											
	2			3			4			5		
$l$	$a_{2,l}$	%	$l$	$a_{3,l}$	%	$l$	$a_{4,l}$	%	$l$	$a_{5,l}$	%	
0.014	0	+7.663[04] -i1.075[04]	99.9	1	+4.906[06] -i6.294[06]	17.2	0	+1.149[09] -i4.849[08]	10.2	1	+1.961[11] +i9.929[11]	31.7
	2	-5.796[03] -i0.416[00]	0.01	3	+3.419[04] -i2.670[07]	82.8	2	+6.563[09] +i1.449[09]	59.4	3	-4.443[11] +i2.012[12]	56.3
							4	+6.453[09] +i1.416[07]	30.4	5	-1.440[09] +i1.191[12]	12.0
0.015	0	+5.437[04] -i2.321[04]	92.6	1	+9.916[06] -i5.235[06]	34.7	0	+9.794[08] +i3.370[08]	12.1	1	-1.290[11] +i7.621[11]	39.3
	2	-3.738[04] -i2.277[01]	7.4	3	+3.951[04] -i2.351[07]	65.3	2	+4.387[09] +i2.594[09]	58.5	3	-5.242[11] +i1.216[12]	49.5
							4	+4.842[09] +i1.422[07]	29.4	5	-2.171[09] +i7.880[11]	11.2
0.017	0	+2.858[04] -i2.188[04]	62.3	1	+8.364[06] -i3.631[06]	39.2	0	+5.220[08] +i4.781[08]	17.3	1	-2.040[11] +i3.229[11]	46.1
	2	-6.264[04] -i1.047[02]	37.7	3	+5.229[04] -i1.735[07]	60.8	2	+2.095[09] +i1.821[09]	53.2	3	-3.054[11] +i4.696[11]	42.5
							4	+2.770[09] +i1.299[07]	29.1	5	-2.569[09] +i3.643[11]	11.4
0.019	0	+1.561[04] -i1.657[04]	37.5	1	+5.651[06] -i2.520[06]	36.2	0	+2.555[08] +i3.411[08]	19.6	1	-1.302[11] +i1.327[11]	49.4
	2	-6.575[04] -i1.780[02]	62.5	3	+5.821[04] -i1.256[07]	63.8	2	+1.073[09] +i1.049[09]	48.5	3	-1.490[11] +i1.998[11]	38.1
							4	+1.633[09] +i1.115[07]	31.9	5	-1.543[09] +i1.788[11]	12.5
0.021	0	+8.710[03] -i1.187[04]	22.4	1	+3.622[06] -i1.768[06]	31.4	0	+1.217[08] +i2.146[08]	19.8	1	-7.299[10] +i5.420[10]	50.3
	2	-6.120[04] -i2.269[02]	77.6	3	+5.767[04] -i9.102[06]	68.6	2	+5.833[08] +i5.838[08]	44.4	3	-7.174[10] +i9.180[10]	35.4
							4	+9.950[08] +i9.007[06]	35.8	5	-1.091[09] +i9.275[10]	14.3
0.023	0	+4.873[03] -i8.251[03]	13.4	1	+2.264[06] -i1.259[06]	26.0	0	+5.631[07] +i1.288[08]	18.6	1	-3.920[10] +i2.180[10]	49.3
	2	-5.442[04] -i2.539[02]	86.6	3	+5.336[04] -i6.666[06]	74.0	2	+3.330[08] +i3.211[08]	40.4	3	-3.460[10] +i4.495[10]	33.7
							4	+6.256[08] +i6.993[06]	41.0	5	-7.161[08] +i5.045[10]	17.0
0.025	0	+2.666[03] -i5.527[03]	07.7	1	+1.371[06] -i9.118[05]	20.5	0	+2.450[07] +i7.460[07]	16.1	1	-2.052[10] +i8.294[09]	46.1
	2	-4.750[04] -i2.650[02]	92.3	3	+4.743[04] -i4.947[06]	79.5	2	+1.982[08] +i1.733[08]	36.3	3	-1.658[10] +i2.323[10]	32.9
							4	+4.049[08] +i5.337[06]	47.6	5	-4.655[08] +i2.863[10]	21.0

TABLE IV. (Continued).

Laser frequency (a.u.)	Number of photons absorbed											
	2			3			4			5		
$l$	$a_{2,l}$	%	$l$	$a_{3,l}$	%	$l$	$a_{4,l}$	%	$l$	$a_{5,l}$	%	
0.026	0	+1.928[03]	5.6	1	+1.043[06]	17.8	0	+1.542[07]	14.3	1	-1.462[10]	43.4
		-i4.414[03]			-i7.818[05]			+i5.567[07]			+i4.872[09]	
	2	-4.423[04]	94.4	3	+4.430[04]	82.2	2	+1.552[08]	34.1	3	-1.134[10]	32.7
		-i2.661[02]			-i4.284[06]		4	+1.250[08]	51.6	5	+i1.701[10]	23.9
0.027												
	0	+1.350[03]	3.8	1	+7.702[05]	15.0	0	+9.160[06]	12.0	1	-1.019[10]	39.5
		-i3.413[03]			-i6.750[05]			+i4.051[07]			+i2.666[09]	
	2	-4.116[04]	96.2	3	+4.117[04]	85.0	2	+1.227[08]	31.8	3	-7.565[09]	32.9
		-i2.651[02]			-3.723[06]		4	+i8.779[07]	56.2	5	+i1.259[10]	27.6
								+2.690[08]			-3.077[08]	
							+i4.038[06]			+i1.687[10]		

the partial detachment rates and angular distributions is valid for lower intensities (approximately, up to  $10^{10}$  W/cm<sup>2</sup>).

In conclusion, the present perturbative Floquet approach provides an accurate description and a computationally efficient procedure for the calculation of multiphoton and above-threshold ionization cross sections in weak and medium strong fields. It should be applicable to a wide range of atomic and molecular multiphoton processes. Application of

the procedure to the study of two- and three-active-electron systems is in progress.

#### ACKNOWLEDGMENTS

This work was partially supported by NSF, under Grant No. PHY-9801889. We acknowledge the support of the Kansas Center for Advanced Scientific Computing for providing the access to the Origin 2000 supercomputer facilities.

- [1] T. N. Rescigno and V. McKoy, Phys. Rev. A **12**, 522 (1975).  
[2] T. N. Rescigno, C. W. McCurdy, and V. McKoy, J. Chem. Phys. **64**, 477 (1976).  
[3] E. Balslev and J. M. Combes, Commun. Math. Phys. **22**, 280 (1971); A. Aguilar and J. M. Combes, *ibid.* **22**, 265 (1971).  
[4] K. T. Chung, Phys. Rev. Lett. **78**, 1416 (1997); Phys. Rev. A **57**, 3518 (1998).  
[5] S. I. Chu and W. P. Reinhardt, Phys. Rev. Lett. **39**, 1195 (1977).  
[6] For reviews on non-Hermitian Floquet methods, see, S. I. Chu, Adv. At. Mol. Phys. **21**, 197 (1985); Adv. Chem. Phys. **73**, 739 (1991).  
[7] S. I. Chu, in *Multiparticle Quantum Scattering with Applications to Nuclear, Atomic, and Molecular Physics*, edited by D. G. Truhlar and B. Simon (Springer, New York, 1997), p. 343.  
[8] A. Maquet, S. I. Chu, and W. P. Reinhardt, Phys. Rev. A **27**, 2946 (1983).  
[9] G. Yao and S. I. Chu, Chem. Phys. Lett. **204**, 381 (1993); J. Wang, S. I. Chu, and C. Laughlin, Phys. Rev. A **50**, 3208 (1994).  
[10] D. A. Telnov and S. I. Chu, Chem. Phys. Lett. **255**, 223 (1996).  
[11] D. A. Telnov and S. I. Chu, Chem. Phys. Lett. **264**, 466 (1997).  
[12] D. A. Telnov and S. I. Chu, Phys. Rev. A **59**, 2864 (1999).  
[13] See, e.g., J. Singh, *Quantum Mechanics: Fundamentals and Applications to Technology* (Wiley, New York, 1997).  
[14] C. Laughlin and S. I. Chu, Phys. Rev. A **48**, 4654 (1993).  
[15] D. A. Telnov, J. Phys. B **24**, 2967 (1991).  
[16] D. A. Telnov and S. I. Chu, J. Phys. B **29**, 4401 (1996).  
[17] D. A. Telnov and S. I. Chu, Phys. Rev. A **50**, 4099 (1994).  
[18] K. R. Lykke, K. K. Murray, and W. C. Lineberger, Phys. Rev. A **43**, 6104 (1991).  
[19] A. W. Wishart, J. Phys. B **12**, 3511 (1979).  
[20] A. L. Stewart, J. Phys. B **11**, 3851 (1978).  
[21] J. Wang, S. I. Chu, and C. Laughlin, Phys. Rev. A **50**, 3208 (1994).  
[22] C. Y. Tang, H. C. Bryant, P. G. Harris, A. H. Mohagheghi, R. A. Reeder, H. Sharifian, H. Tootouchi, C. R. Quick, J. B. Donahue, S. Cohen, and W. W. Smith, Phys. Rev. Lett. **66**, 3124 (1991).  
[23] X. M. Zhao, M. S. Gulley, H. C. Bryant, C. E. M. Strauss, D. J. Funk, A. Stintz, D. C. Rislove, G. A. Kyrala, W. B. Ingalls, and W. A. Miller, Phys. Rev. Lett. **78**, 1656 (1997).  
[24] L. Præstegaard, T. Andersen, and P. Balling, Phys. Rev. A **59**, R3154 (1999).  
[25] A. Dalgarno and J. T. Lewis, Proc. R. Soc. London, Ser. A **233**, 70 (1955).